Plasmodium falciparum GCN5 plays a key role in regulating artemisinin resistance–related stress responses

Ahmad Rushdi Shakri[1#], Chengqi Wang[2#], Amuza Byaruhanga Lucky[1], Mohammad Kalamuddin[1], Anongruk Chim-Ong[1], Xiaolian Li[1], Liwang Cui[1,2], Jun Miao[1,2*]

1. Department of Internal Medicine, Morsani College of Medicine, University of South Florida, 3720 Spectrum Blvd, Tampa, FL 33612, USA

2. Center for Global Health and Infectious Diseases Research, College of Public Health, University of South Florida, 3720 Spectrum Blvd, Tampa, FL 33612, USA

Running title: PfGCN5 functions in stress response and ART resistance

[#] These authors contributed equally to this work.

*** Correspondence:**

Jun Miao

Phone: 813-973-7374

Email: jmiao1@usf.edu

ABSTRACT

Plasmodium falciparum causes the most severe malaria and is exposed to various environmental and physiological stresses in the human host. Given that GCN5 plays a critical role in regulating stress responses in model organisms, we aimed to elucidate PfGCN5's function in stress responses in *P. falciparum*. With TetR-DOZI conditional knockdown (KD) system, we successfully down-regulate PfGCN5 and found that KD parasites became more sensitive to heat shock, low glucose starvation, and dihydroartemisinin (DHA), the active metabolite of all artemisinin (ART) compounds. Transcriptomic analysis via RNA-seq identified 300-400 genes involved in PfGCN5-dependent, general, and stress-specific responses with high levels of overlaps among three stress conditions. Notably, using ring-stage survival assay (RSA), we found that KD or inhibition of PfGCN5 could sensitize the ART-resistant parasites to the DHA treatment. All these indicate that PfGCN5 is pivotal in regulating general and stress-specific responses in malaria parasites, implicating PfGCN5 as a potential target for malaria intervention.

IMPORTANCE Malaria leads to about half a million deaths annually and these casualties were majorly caused by the infection of *Plasmodium falciparum*. This parasite strives to survive by defending against a variety of stress conditions, such as malaria cyclical fever (heat shock), starvation due to low blood sugar (glucose) levels (hypoglycemia), and drug treatment. Previous studies have revealed that *P. falciparum* has developed unique stress responses to different stresses including ART treatment, and ART-resistant parasites harbor elevated stress responses. In this study, we provide critical evidence on the role of PfGCN5, a histone modifier, and a chromatin coactivator, in regulating general and stress-specific responses in malaria parasites, indicating that PfGCN5 can be used as a potential target for anti-malaria intervention.

INTRODUCTION

Malaria is one of the most severe public health problems worldwide. *Plasmodium falciparum* causes the most severe form of malaria and is responsible for about half a million deaths annually [1]. Malaria parasites are exposed to various environmental and physiological stresses in the human host (e.g., cyclical fever, low nutrition, and drug treatment) [2]. They have evolved general and specific mechanisms to defend against those assaults [3-5]. Several chaperones (PfHSP70-1, PfHSP70-x, PfHSP110, and the endoplasmic reticulum chaperone PfGRP170) were identified as essential proteins for the parasite to respond to heat shock (HS) [6-10]. PfAP2-HS, an ApiAP2 (AP2) domain-containing transcription factor, was found to rapidly activate *Pfhsp70-1* and *Pfhsp90* in the protective HS response [5]. Besides the conserved mechanisms for tolerance to febrile temperature and oxidative stress such as redox and protein-damage responses, parasites developed specific mechanisms such as regulating isoprenoid biosynthesis and its downstream protein modifications (geranylgeranylation and farnesylation) [4, 11]. Isoprenoid biosynthesis occurs in the apicoplast, an apicomplexan pathogen-specific organelle derived from an algal endosymbiont plastid. Many genes targeting the apicoplast were also up regulated upon HS, suggesting that the parasite utilizes an analogous defense system against heat stresses like plants [4, 12, 13].

Malaria parasites employ similar mechanisms to deal with the stresses from antimalarial treatment. ART, the first line of the anti-malaria drug, causes the production of free radical species, including reactive oxygen species (ROS), which damage proteins, lipids, and DNA [14-25]. Low-dose ART treatment was found to activate the response pathways critical for the tolerance to febrile temperature [4]. ART-resistant parasites with mutations in the Kelch protein 13 (PfK13) up-regulated genes related to stress responses (e.g., protein folding, redox, and proteasome-linked protein turnover). ART-resistant parasites respond to ART treatment by elevating gene expression related to apicoplast and mitochondrial metabolism, vesicular trafficking, lipid transport, and tRNA modifications [21-25].

GCN5 is a well-known key regulator of stress responses in the human, plants, yeast, and *Toxoplasma* by coordinating with specific transcriptional factors [26-33]. Recent studies also identified up-regulation of PfGCN5 in response to stress conditions (ART treatment, glucose starvation, and HS) along with many other up-regulated genes in *P. falciparum* [3, 34].

Intriguingly, PfGCN5 was found to bind many of these genes, but most of the binding sites were localized in the coding regions, not in promoters. Treatment with garcinol, a PfGCN5 inhibitor, sensitized the ART-resistant *P. falciparum* parasite to ART during the ring stage. In addition, treating parasites with ART caused substantial changes in the abundance of active chromatin markers H3K9ac and H4K8ac [35]. Collectively, these studies provided tangential evidence implying PfGCN5's participation in responses to ART.

To elucidate the functions of PfGCN5 in orchestrating the transcriptional program in *P. falciparum*, we deleted the C-terminal bromodomain of PfGCN5, which supposedly mediates the binding of PfGCN5 to acetylated lysines. This has led to drastic transcriptional changes in many genes, including protein folding-related genes and *AP2-HS* [36], suggesting that PfGCN5 regulates the stress response pathways. However, this assumption is undermined by the dislocation of the PfGCN5 complex from its chromatin targets due to bromodomain deletion. To elucidate PfGCN5's critical role in regulating stress responses in *P. falciparum*, we employed a conditional knockdown (KD) system to down-regulate PfGCN5 and determined the parasite's responses to different stress conditions. We provide critical evidence about the role of PfGCN5 in regulating general and stress-specific responses in malaria parasites, implicating PfGCN5 as a potential target for therapeutic development.

RESULTS

Conditional KD of PfGCN5 impairs parasite growth

PfGCN5 is essential for asexual blood stages, and deletion of the C-terminal bromodomain led to a defect in RBC invasion and dysregulated expression of virulence genes [36]. To elucidate whether and how PfGCN5 regulates stress responses, we employed the TetR-DOZI system [37, 38] to conditionally knock down PfGCN5 expression. We created a parasite line, TetR-PfGCN5::GFP, with the insertion of the 10× aptamer in the 3' end of the endogenous PfGCN5 locus and fusion of the GFP tag to the PfGCN5 C-terminus, which would allow us to monitor PfGCN5 expression (**Figure 1A, S1A**). Correct integration of the plasmid at the *PfGCN5* locus was confirmed by a genomic Southern blot (**Figure S1B**). The binding of the TetR-DOZI to the

aptamer in the presence of anhydrous tetracycline (+aTc) allowed the expression of PfGCN5-GFP, whereas withdrawal of aTc (-aTc) for one intraerythrocytic developmental cycle (IDC) led to ~50% reduction of PfGCN5-GFP expression, shown in GFP fluorescence intensity by flow cytometry analysis (**Figure 1A, 1B**). Intriguingly, the withdrawal of aTc beyond one IDC did not further reduce the PfGCN5 expression level (**Figure S1C**), suggesting that parasites were probably restrained from further reduction of PfGCN5 expression due to its essentiality. The -aTc parasites grew significantly more slowly starting from the second cycle than the +aTc parasites (**Figure 1C**). We found that PfGCN5 KD was reversible, as within ~10 h of aTc add-back, the growth rate of the parasites was rapidly restored and PfGCN5-GFP expression returned to the level of the +aTc culture (**Figure S1C, S1D**).

PfGCN5 KD renders parasites more sensitive to stresses

To investigate if PfGCN5 is involved in regulating stress responses, the TetR-PfGCN5::GFP parasite line cultured with or without aTc was treated at the early ring stage with different stress conditions: HS (41 ºC for 6 h), low glucose (0.5 g/L for 6 h), or DHA (1 μM for 12 h) (**Figure 1D-F**). After removing the stress conditions, aTc was added back to the culture, and parasite growth was monitored daily. TetR-PfGCN5::GFP parasites without aTc grew significantly more slowly than +aTc parasites under HS and low-glucose conditions (**Figure 1D, 1E**). After DHA treatment, both +aTc and -aTc parasites were non-detectable through day 9. The +aTc culture resumed growth and reached 5% parasitemia on day 15, whereas the -aTc culture had a 4-day delay in reaching 5% parasitemia (**Figure 1F**). This delayed growth phenotype was not caused by aTc because the 3D7 WT parasite treated the same way showed the same growth pattern after DHA treatment (**Figure S1E**). Taken together, PfGCN5 KD reduced the parasite's tolerance to different stresses, directly linking PfGCN5 to regulating stress responses.

Parasites apply general and specific responses to different stresses

To determine how the parasites respond to different stress conditions, we first characterize the transcriptomic changes of TetR-PfGCN5::GFP parasites (+aTc) at the ring-stage (6 h post-invasion, hpi) after treatment with HS (41ºC), low glucose (0.5 g/L), or DHA (30 nM) for 6 h. Transcriptomic analysis was performed by RNA-seq with three biological replicates. DESeq2

analysis using a cutoff of > 1.5-fold and *p-adj* < 0.1 [39] identified 1183, 1130, and 1038 up-regulated, as well as 1151, 1126, and 1049 down-regulated genes by HS, low-glucose, and ART treatment, respectively (**Figure 2A-C, Table S1**). Surprisingly, there were substantial overlaps in the up-and down-regulated genes among different stress conditions (57-65% in the up-regulated genes and 70-76% in the down-regulated genes) (**Figure 2D and E, Table S1**). Gene ontology (GO) enrichment analysis based on biological process (BP) (**Figure 2F**) and cellular component (CC) (**Figure S2A**) showed that genes related to translation and tRNA metabolism, protein-damage responses (protein folding and proteasome), glycolysis and gluconeogenesis, nucleotide metabolism, host-cell remodeling, and mitochondrial and apicoplast proteins were up-regulated in all stress conditions. In contrast, genes related to merozoite invasion, egression, DNA replication, cytoskeleton, protein phosphorylation, and phospholipid transport were downregulated, indicating that parasites used a general stress response to different stress conditions (**Figure 2G, S2B**). Partial ART resistance in *P. falciparum* is medicated by mutations in the propeller domain of PfK13, and the expression levels of PfK13-interacting proteins (KICs) were found to influence hemoglobin uptake [40]. Intriguingly, PfK13 and seven of ten KICs (KIC1-3, 5-8) were significantly down-regulated in all three stress conditions, whereas KIC4 was significantly down-regulated under low glucose and KIC10 was down-regulated by both low-glucose and DHA treatments (**Table S1**).

Transcriptomic analysis also revealed many genes whose expression was altered in a stress condition-specific manner (**Figure 2F, 2G, S2A and S2B**). HS specifically induced the up-regulation of genes related to the response to heat and protein unfolding, including *Pfhsp70-1* and *Pfhsp90*, which are regulated by the transcription factor PfAP2-HS [5]. The low-glucose condition specifically activated genes related to oxidative stress response and mitochondrial ATP synthesis. ART treatment specifically up-regulated genes related to cell-cycle regulation and ER stress response. Genes related to protein geranylgeranylation (apicoplast function) were only enriched after HS and ART treatment but not under glucose starvation (**Figure 2F**, **Table S1**). Collectively, these data indicate that different stress conditions induce specific stress responses in malaria parasites.

PfGCN5 plays a crucial role in the regulation of stress responses

To understand how PfGCN5 is involved in stress responses, we sought to determine the transcriptomic changes of the parasites after manipulating PfGCN5 expression in response to different stress conditions. Transcriptomic analysis of the TetR-PfGCN5::GFP parasite at the ring stage only identified two genes (*PfGCN5* and *EBA175*) that were significantly down-regulated (> 1.5-fold, *p-adj* < 0.1) after PfGCN5 KD (-aTc), indicating that reduced PfGCN5 expression did not disturb the overall transcription program at the ring stage (**Table S2**). We then subjected the -aTc TetR-PfGCN5::GFP parasites at 6 hpi to the same stress conditions for +aTc TetR-PfGCN5::GFP parasites mentioned above for 6 h and harvested RNA for RNA-seq analysis. In the -aTc parasites, the stress conditions HS, low glucose, and ART treatment resulted in a similar number of genes with expression changes as in the +aTc parasites (**Figure 2**): 971, 1136, and 911 up-regulated genes and 922, 1170, and 1041 down-regulated genes, respectively. These genes showing altered expression also overlapped substantially, with 48-60% and 66-84% overlaps among the up-and down-regulated genes, respectively (**Figure 3A, 3B**, **Table S3**).

Comparison of the transcriptomes between the -aTc and +aTc parasites allowed us to identify 2825, 2738, and 2528 genes that were differentially regulated by the HS, low glucose, and DHA treatment, respectively (**Table S4**). Based on their expression patterns, these genes were grouped into five clusters (**Figure 3C, Table S4**), while HS included an additional cluster (VI). Cluster I and II genes were significantly down-regulated and failed to be up-regulated in -aTc parasites compared to +aTc parasites under three stress conditions, respectively, suggesting that these two clusters are likely the PfGCN5-dependent stress-response genes (**Figure 3C**). The genes in clusters I and II are involved in many aspects of critical pathways such as translation (ribosome biogenesis and tRNA modification), H3K4me3 modification, glutamine metabolism, energy metabolism (ATP metabolism, glycolysis, and gluconeogenesis), drug response (ART proteome, xenobiotic stimulus), protein trafficking (ER and PTEX translocon) and digestion (food vacuole) (**Figure 3D**). Notably, KIC4, which was down-regulated only after glucose starvation in +aTc parasites, was significantly down-regulated in -aTc parasites under all three stress conditions. Similarly, GARP (glutamic acid-rich protein) expressed on the surface of parasite-infected RBC [41, 42] also failed to be up-regulated in -aTc parasites under three stress conditions (**Figure 3D**). Antibodies against GARP killed the parasites and were positively associated with protection against severe malaria in children [43].

Conversely, cluster III genes, down-regulated in the +aTc parasites, were up-regulated in the -aTc parasites under three stress conditions, probably to compensate for PfGCN5 KD (**Figure 3D**). These include genes related to DNA replication and repair, cell cycle, and isoprenoid biosynthesis. Similarly, some genes were up-regulated only by glucose starvation (cell adhesion and cytoskeleton) and HS (mitochondrion electron transport). A large number of genes belong to clusters IV and V, which were up- and down-regulated in the -aTc parasites under stress conditions in the same trends as in the +aTC parasite, respectively, suggesting that these genes may be PfGCN5-independent. HS induced a new cluster of genes (VI), which were up-regulated in the -aTc parasites but no change in the +aTc parasites (**Figure 3C**). These genes are involved in similar pathways as the cluster III genes, suggesting that HS might have involved more genes in compensation for PfGCN5 KD (**Table S4**). By comparing the overlaps within these clusters upon three different stress conditions, low levels of overlaps were found among PfGCN5-dependent stress-response genes (cluster I and II) and the KD compensation-related genes (cluster III), whereas high levels of overlaps among the PfGCN5-independent stress-response genes (cluster IV and V) were identified (**Figure S3, Table S4**), suggesting PfGCN5-dependent stress responses are also stress-condition-specific to a certain degree. Genes related to the HSP70 cycle, P-bodies, and translation initiation were down-regulated (cluster I) in -aTc parasites specifically under glucose starvation, while genes related to protein geranylgeranylation, isoprenoid biosynthesis, proteasome assembly, and mitochondrion transport and targeting failed to be up-regulated in -aTc parasites under DHA treatment. Likewise, genes related to cation homeostasis (pH reduction) and hemoglobin digestion failed to be up-regulated in -aTc parasites under low glucose and HS, respectively (**Figure 3D**). Collectively, these data demonstrate that PfGCN5 regulates stress response by targeting general and stress condition-specific stress response genes.

PfGCN5 KD reduces parasites' tolerance to DHA treatment

Growth recovery assay and transcriptomic analysis after DHA treatment indicated PfGCN5's involvement in regulating general and specific responses to DHA (**Figure 1F, 3D**). To translate this phenotype into ART sensitivity, we performed the ring-stage survival assay (RSA) with TetR-PfGCN5::GFP parasites. The TetR-PfGCN5::GFP (-aTc) parasites at the early ring were

exposed to 700 nM DHA for 6 h, and aTc was added back right after DHA treatment to exclude the subsequent effect of PfGCN5 KD on parasite growth defect. Compared to the RSA value of the TetR-PfGCN5::GFP parasites under the +aTc conditions, PfGCN5 KD resulted in a ~60% reduction in the RSA value (**Figure 4A**).

With the demonstration of PfGCN5's role in regulating parasite's responses to ART drugs, we wanted to test if inhibition of PfGCN5's enzymatic activity would re-sensitize ART-resistant parasites to ART drugs. We evaluated butyrolactone 3 (MB-3), which we showed previously to inhibit PfGCN5's enzymatic activity with an IC_{50} of ~125 μM [44]. With the standard SYBR green I growth inhibition assay, MB-3 inhibited 3D7 parasites at an IC_{50} of ~ 27.5 μM. We found that a 6-h exposure of Cam2, an ART-resistant strain collected from Cambodia with the K13 C580Y mutation (MRA-1236), at the early-ring stage to 10.9, 17.3, and 27.5 μM of MB-3, corresponding to the IC_{10}, IC_{25}, and IC_{50} concentrations of the drug, respectively, did not cause noticeable changes in the survival rate of ART-resistant strain as compared to the DMSO vehicle control (**Figure 4B**). Whereas RSA of Cam2 showed a survival rate of 13%, co-incubation of DHA and MB-3 for 6 h significantly reduced the RSA value in an MB-3 concentration-dependent manner compared to DHA treatment only (**Figure 4D**). Taken together, these data showed that KD or inhibition of PfGCN5 could re-sensitize the ART-resistant parasites to ART drugs.

DISCUSSION

This study aimed to confirm PfGCN5's involvement in regulating stress responses in the malaria parasite and gain a mechanistic understanding of PfGCN5's role in responding to different stress conditions. Using a conditional KD system, we successfully down-regulated PfGCN5 expression and showed that PfGCN5 KD increased the parasite's susceptibility to all stress conditions used, emphasizing PfGCN5's central role in stress response. Through transcriptomic analysis, we identified 300-400 genes involved in PfGCN5-dependent, general, and stress-specific responses. Furthermore, using growth recovery assay and RSA, we found that KD or inhibition of PfGCN5 could sensitize the ART-resistant parasites to the ART treatment.

In addition to the parasite-specific functions of PfGCN5 in regulating invasion and virulence in *P. falciparum*, we confirm an evolutionarily conserved role of PfGCN5 in regulating

stress responses. We have shown that the malaria parasites can mount a rapid stress response, with the expression of >2,000 genes altered under each stress condition tested. Importantly, there were significant overlaps in the differentially expressed genes among the different stresses, highlighting the presence of a shared general mechanism. By comparing gene expression between PfGCN5-normal and PfGCN5-deficient parasites exposed to stresses, we identified a subset of 300-400 genes whose expression in response to stresses depended on PfGCN5. These genes are involved in common stress responses (e.g., translation and ribosome, tRNA, and ATP metabolic process, glycolysis, gluconeogenesis, protein geranylgeranylation, proteasome assembly, Sec61 translocon, isoprenoid biosynthesis, food vacuole, apoptosis, and mitochondrion targeting) and stress-specific response (e.g., P-bodies, protein folding, and mitochondrion targeting upon starvation, HS, and ART treatment, respectively). Especially, seven K13-interacting proteins (KICs) involved in ART resistance by participating in hemoglobin uptake [40] were down-regulated under all three stress conditions. Furthermore, KIC4 was dysregulated in PfGCN5 KD parasites during stress, indicating that the K13 regulatory pathway is a common stress response. Similarly, a large-scale forward-genetic screen in *P. falciparum* revealed apicoplast-targeted proteins including isoprenoid biosynthesis and its downstream protein modifications (geranylgeranylation and farnesylation) as a common pathway mediating tolerance to febrile temperature, a low dose of ART, and oxidative stress [4, 11]. Likewise, ART-resistant parasites showed elevated stress responses [4, 21-25]. In addition, this study also identified stress-specific responses, such as upregulation of *Pfhsp70-1* and *Pfhsp90* after HS, ATP synthesis under starvation, and ER stress response after ART treatment. These data highlight that the malaria parasite has evolved an integrated mechanism responding to different stress conditions, and PfGCN5 is a key activator of general and specific stress responses.

PfGCN5 is present in a large coactivator protein complex(es) to regulate global gene expression in *P. falciparum* [36]. Activation of specific pathways by PfGCN5 may be conferred by specific transcription factors such as the AP2-domain proteins. In the PfGCN5 complex, PfAP2-LT is present as a consistent member, and other AP2 TFs (e.g., AP2-I and PF3D7_1239200) have also been found in PfGCN5 pulldowns [36, 45]. Of particular relevance, PfAP2-HS was found to play a key role in the HS response through the activation of *Pfhsp70-1* and *Pfhsp90* [5]. While we hypothesize that the PfGCN5 complex may be dynamically recruited

297 to activate genes in the stress response pathways by PfAP2-HS, the exact mechanism remains to
298 be tested.

299 The finding of PfGCN5 KD resulting in delayed recovery and lower RSA rate upon DHA
300 exposure is consistent with the reflection of the partial ART resistance phenotype in the general
301 elevation of stress tolerance as typically occurring in an early phase of resistance [46]. Re-
302 sensitization of the ART-resistant parasites by chemically inhibiting PfGCN5 may provide a way
303 to deal with the emerging problem of ART resistance in endemic areas and underline PfGCN5 as
304 a potential target for therapeutic development.

305

306 # MATERIAL AND METHODS

307 ## Parasite culture

308 The *P. falciparum* strain 3D7 and its genetically modified clones were cultured at 37°C in a gas
309 mixture of 5% CO_2, 3% O_2 and 92% N_2 with type O^+ RBCs at 5% hematocrit in RPMI 1640
310 medium supplemented with 25 mM $NaHCO_3$, 25 mM HEPES, 50 mg/L hypoxanthine, 2 g/L
311 glucose, 0.5% Albumax II and 40 mg/ml gentamicin sulfate [47]. Synchronization of asexual
312 stages was performed by sorbitol treatment at the rings stage followed by incubation of
313 synchronized schizonts with fresh RBCs for 3 h to obtain highly synchronized ring-stage
314 parasites [48].

315 ## Genetic manipulation of *PfGCN5*

316 To generate a PfGCN5 KD parasite line by TetR-DOZI system, a *PfGCN5* fragment [nucleotides
317 (nt) 3778-4758] was amplified using primers F1 (GAGCGCGCTGTTACCTCAACTGAGC,
318 *BssH*II underlined) and R1 (GAGGTTACCTGCTGTATCAGTTATAGCTTC, *BstE*II
319 underlined) from *P. falciparum* genomic DNA and cloned into pMG75 ATPase4 plasmid [37,
320 38] to replace the ATPase4 fragment and generate pMG75-PfGCN5. To fuse the C-terminal of
321 PfGCN5 with GFP, we amplified GFP using primers F2
322 (CAGGTTACCATGAGTAAAGGAGAAGAACTTTTC, *BstE*II underlined) and R2
323 (CTGACGTCTTATTTGTATAGTTCATCCATGCC, *Aat*II underlined) and cloned it into
324 pMG75-PfGCN5 at the *BstE*II and *Aat*II sites.

325 Parasite transfection was done using the RBC loading method [49]. Briefly, 100 µg of

plasmid was introduced into fresh RBCs by electroporation. Purified schizonts were used to infect the RBCs pre-loaded with the plasmid, and selection was done with blasticidin (BSD) at 2.5 µg/mL for approximately 4 weeks with weekly replenishment of fresh RBCs until resistant parasites appeared. Resistant parasites were subjected to three cycles of drug on-off selection and single clones of parasites with stable integration of the constructs were obtained by limiting dilution [48]. aTc at 0.5 µM was constantly added to the culture to maintain adequate expression of *PfGCN5*. GFP-positive parasites were sorted and cloned by fluorescence-activated cell sorting. Correct integrations of plasmids into the parasite genome were screened by Southern blot with the digoxigenin (DIG)-labeled probes using an established protocol [36, 50]. The probe was generated by using the F1 and R1 primers.

PfGCN5 KD and growth phenotype analysis

Flow cytometry was used to measure the GFP level in the TetR-PfGCN5::GFP parasites. The growth of the TetR-PfGCN5::GFP parasite line was measured in triplicate. Cultures were tightly synchronized, as described above. The parasitemia of culture was monitored daily by microscopy of Giemsa-stained blood smears. Growth rates after *PfGCN5* KD were analyzed by starting cultures at 0.1% rings with the vehicle control (ethanol, -aTc) or aTc (+aTc) for seven days. Growth rates after HS and low glucose treatment (6 h) were measured by starting cultures at 0.5% rings with the vehicle control (-aTc) or aTc for five days. Parasite recovery assay was performed as described previously by treating 2% early ring-stage parasites with 1 µM of DHA for 12 h [51]. aTc was added back to the PfGCN5 KD (-aTc) culture after removing stress conditions.

Transcriptome analysis

To compare the parasites' transcriptomes upon stress conditions, we performed RNA-seq analysis using the ring-stage TetR-GCN5::GFP parasites with or without aTc. The experiment was done in 2-3 replicates. Total RNA was extracted using the ZYMO RNA purification kit and RNA integrity was confirmed by the TapeStation system (Agilent). Total RNA was used to generate the sequencing libraries using the KAPA Stranded mRNA Seq kit for the Illumina sequencing platform according to the manufacturer's protocol (KAPA biosystems). Libraries were sequenced on an Illumina NextSeq 550 using 150 nt paired-end sequencing. Reads from Illumina sequencing were mapped to the *P. falciparum* genome sequence (Genedb v3.1) using

HISAT2 [52]. The expression levels and the differential expression were calculated by FeatureCounts and DESeq2 [53, 54] with the criteria of ≥ 1.5-fold of alteration and *p*-adjustment <0.1. RNA-seq data were submitted to the NCBI GEO repository (accession number GSE221211) with a token (cxmngauyrvcfjqj) for reviewers' accession.

GO enrichment analysis and clustering

The GO enrichment was performed on PlasmDB (https://plasmodb.org/plasmo/). The fold changes of gene expressions were further normalized by Z-score, and K-means were performed to identify differential gene expression patterns among the transcriptomes with or without KD of PfGCN5 under different stress conditions.

In vitro drug assay and RSA

The standard SYBR Green I-based fluorescence assay [55, 56] was used to assess parasite susceptibilities to MB-3. Synchronized cultures at the ring stage were diluted with fresh complete medium to 1% hematocrit and 0.5% parasitemia. *In vitro* drug assays were performed in 96-well microtiter plates with serially diluted drug concentrations. Three technical and biological replications were performed.

RSA was performed as previously described [56-60]. Briefly, schizonts were purified from tightly synchronized cultures using a Percoll gradient and allowed to rupture and invade fresh RBCs for 3 h. The cultures were treated with sorbitol to select early rings and eliminate the remaining schizonts. Ring-stage parasites of 0-3 hpi at 1% parasitemia and 1% hematocrit were exposed to 700 nM DHA for 6 h, followed by a single wash. MB-3 was added and washed simultaneously as DHA, and aTc was added back to the PfGCN5 KD (-aTc) culture after drug treatment. After culturing for 66 h, ~10,000 RBCs were observed on thin blood smears to count viable parasites.

Statistical analysis

For all experiments, three or more independent biological replicates were performed. The results were presented as mean ± SD. Results were regarded as significant if $P < 0.05$ as established by T-test, and the respective analysis was shown in the figure legends.

Acknowledgments

This study was supported by the startup fund from Morsani College of Medicine, University of South Florida, and grant R21AI149202 from the National Institute of Allergy and Infectious Diseases (NIAID), NIH, USA to JM, and grants R01AI128940 and U19AI089672 from NIAID, NIH, USA to LC. We are grateful to Jacobus *Pharmaceuticals* for providing the drug WR99210. We thank the University of South Florida Genomics Program (Sequencing Core and Computational Core/Omics Hub) for supporting NGS sequence and data analysis.

Author Contributions

J.M. conceived and designed the study. AR.S, C.W., and AB.L. performed research, acquired and analyzed data. C.W. analyzed the RNA-seq data. M.K. and A.C. assisted research. X.L. conducted parasite culture and phenotypic growth analysis. J.M. wrote the original draft. L.C. revised the manuscript.

Declaration of Interests

The authors declare no competing interests.

REFERENCES

1. WHO, *Would Malaria Report 2021.* Geneva: WHO, 2021.
2. Brown, A.C. and J.L. Guler, *From Circulation to Cultivation: Plasmodium In Vivo versus In Vitro.* Trends in Parasitology, 2020. **36**(11): p. 914-926.
3. Rawat, M., et al., *Histone acetyltransferase PfGCN5 regulates stress responsive and artemisinin resistance related genes in Plasmodium falciparum.* Sci Rep, 2021. **11**(1): p. 852.
4. Zhang, M., et al., *The apicoplast link to fever-survival and artemisinin-resistance in the malaria parasite.* Nat Commun, 2021. **12**(1): p. 4563.
5. Tinto-Font, E., et al., *A heat-shock response regulated by the PfAP2-HS transcription factor protects human malaria parasites from febrile temperatures.* Nat Microbiol, 2021. **6**(9): p. 1163-1174.
6. Dutta, T., et al., *Exported plasmodial J domain protein, PFE0055c, and PfHsp70-x form a specific co-chaperone-chaperone partnership.* Cell Stress & Chaperones, 2021. **26**(2): p. 355-366.
7. Day, J., et al., *The Plasmodium falciparum Hsp70-x chaperone assists the heat stress response of the malaria parasite.* Faseb Journal, 2019. **33**(12): p. 14611-14624.
8. Kudybah, H.M., et al., *The endoplasmic reticulum chaperone PfGRP170 is essential for asexual development and is linked to stress response in malaria parasites.* Cellular Microbiology, 2019. **21**(9).
9. Lu, K.Y., et al., *Phosphatidylinositol 3-phosphate and Hsp70 protect Plasmodium falciparum from heat-induced cell death.* Elife, 2020. **9**.

10. Muralidharan, V., et al., *Plasmodium falciparum heat shock protein 110 stabilizes the asparagine repeat-rich parasite proteome during malarial fevers.* Nature Communications, 2012. **3**.
11. Mathews, E.S., A.J. Jezewski, and A.R.O. John, *Protein Prenylation and Hsp40 in Thermotolerance of Plasmodium falciparum Malaria Parasites.* Mbio, 2021. **12**(3).
12. Boucher, M.J., et al., *Integrative proteomics and bioinformatic prediction enable a high-confidence apicoplast proteome in malaria parasites.* Plos Biology, 2018. **16**(9).
13. Foth, B.J., et al., *Dissecting apicoplast targeting in the malaria parasite Plasmodium falciparum.* Science, 2003. **299**(5607): p. 705-708.
14. Haynes, R.K., et al., *Considerations on the mechanism of action of artemisinin antimalarials: part 1--the 'carbon radical' and 'heme' hypotheses.* Infect Disord Drug Targets, 2013. **13**(4): p. 217-77.
15. Heller, L.E. and P.D. Roepe, *Artemisinin-Based Antimalarial Drug Therapy: Molecular Pharmacology and Evolving Resistance.* Trop Med Infect Dis, 2019. **4**(2).
16. Klonis, N., D.J. Creek, and L. Tilley, *Iron and heme metabolism in Plasmodium falciparum and the mechanism of action of artemisinins.* Curr Opin Microbiol, 2013. **16**(6): p. 722-7.
17. Heller, L.E., E. Goggins, and P.D. Roepe, *Dihydroartemisinin-Ferriprotoporphyrin IX Adduct Abundance in Plasmodium falciparum Malarial Parasites and the Relationship to Emerging Artemisinin Resistance.* Biochemistry, 2018. **57**(51): p. 6935-6945.
18. Gopalakrishnan, A.M. and N. Kumar, *Antimalarial action of artesunate involves DNA damage mediated by reactive oxygen species.* Antimicrob Agents Chemother, 2015. **59**(1): p. 317-25.
19. Krungkrai, S.R. and Y. Yuthavong, *The antimalarial action on Plasmodium falciparum of qinghaosu and artesunate in combination with agents which modulate oxidant stress.* Trans R Soc Trop Med Hyg, 1987. **81**(5): p. 710-4.
20. Wang, J., et al., *Artemisinin directly targets malarial mitochondria through its specific mitochondrial activation.* PLoS One, 2010. **5**(3): p. e9582.
21. Mok, S., et al., *Artemisinin-resistant K13 mutations rewire Plasmodium falciparum's intra-erythrocytic metabolic program to enhance survival.* Nat Commun, 2021. **12**(1): p. 530.
22. Mok, S., et al., *Population transcriptomics of human malaria parasites reveals the mechanism of artemisinin resistance.* Science, 2015. **347**(6220): p. 431-435.
23. Bridgford, J.L., et al., *Artemisinin kills malaria parasites by damaging proteins and inhibiting the proteasome.* Nature Communications, 2018. **9**.
24. Rocamora, F., et al., *Oxidative stress and protein damage responses mediate artemisinin resistance in malaria parasites.* Plos Pathogens, 2018. **14**(3).
25. Cui, L., et al., *Mechanisms of in vitro resistance to dihydroartemisinin in Plasmodium falciparum.* Mol Microbiol, 2012. **86**(1): p. 111-28.
26. Gaupel, A.C., T.J. Begley, and M. Tenniswood, *Gcn5 Modulates the Cellular Response to Oxidative Stress and Histone Deacetylase Inhibition.* J Cell Biochem, 2015. **116**(9): p. 1982-92.
27. Hu, Z., et al., *Histone acetyltransferase GCN5 is essential for heat stress-responsive gene activation and thermotolerance in Arabidopsis.* Plant J, 2015. **84**(6): p. 1178-91.
28. Johnsson, A., et al., *Stress-specific role of fission yeast Gcn5 histone acetyltransferase in programming a subset of stress response genes.* Eukaryot Cell, 2006. **5**(8): p. 1337-46.
29. Naguleswaran, A., et al., *Toxoplasma gondii lysine acetyltransferase GCN5-A functions in the cellular response to alkaline stress and expression of cyst genes.* PLoS Pathog, 2010. **6**(12): p. e1001232.
30. Mutlu, B. and P. Puigserver, *GCN5 acetyltransferase in cellular energetic and metabolic processes.* Biochimica Et Biophysica Acta-Gene Regulatory Mechanisms, 2021. **1864**(2).
31. Gan, L., et al., *Updated Mechanisms of GCN5-The Monkey King of the Plant Kingdom in Plant Development and Resistance to Abiotic Stresses.* Cells, 2021. **10**(5).

32. Xue-Franzen, Y., et al., *Genome-wide characterisation of the Gcn5 histone acetyltransferase in budding yeast during stress adaptation reveals evolutionarily conserved and diverged roles.* Bmc Genomics, 2010. **11**.
33. Hsieh, W.C., et al., *Glucose starvation induces a switch in the histone acetylome for activation of gluconeogenic and fat metabolism genes.* Mol Cell, 2022. **82**(1): p. 60-74 e5.
34. Rawat, M., et al., *Role of PfGCN5 in nutrient sensing and transcriptional regulation in Plasmodium falciparum.* J Biosci, 2020. **45**.
35. Gupta, D.K., et al., *DNA damage regulation and its role in drug-related phenotypes in the malaria parasites.* Sci Rep, 2016. **6**: p. 23603.
36. Miao, J., et al., *A unique GCN5 histone acetyltransferase complex controls erythrocyte invasion and virulence in the malaria parasite Plasmodium falciparum.* PLoS Pathog, 2021. **17**(8): p. e1009351.
37. Goldfless, S.J., J.C. Wagner, and J.C. Niles, *Versatile control of Plasmodium falciparum gene expression with an inducible protein-RNA interaction.* Nat Commun, 2014. **5**: p. 5329.
38. Ganesan, S.M., et al., *Synthetic RNA-protein modules integrated with native translation mechanisms to control gene expression in malaria parasites.* Nat Commun, 2016. **7**: p. 10727.
39. Love, M.I., W. Huber, and S. Anders, *Moderated estimation of fold change and dispersion for RNA-seq data with DESeq2.* Genome Biol, 2014. **15**(12): p. 550.
40. Birnbaum, J., et al., *A Kelch13-defined endocytosis pathway mediates artemisinin resistance in malaria parasites.* Science, 2020. **367**(6473): p. 51-59.
41. Davies, H.M., K. Thalassinos, and A.R. Osborne, *Expansion of Lysine-rich Repeats in Plasmodium Proteins Generates Novel Localization Sequences That Target the Periphery of the Host Erythrocyte.* Journal of Biological Chemistry, 2016. **291**(50): p. 26188-26207.
42. Almukadi, H., et al., *Human erythrocyte band 3 is a host receptor for Plasmodium falciparum glutamic acid-rich protein.* Blood, 2019. **133**(5): p. 470-480.
43. Raj, D.K., et al., *Anti-PfGARP activates programmed cell death of parasites and reduces severe malaria.* Nature, 2020. **582**(7810): p. 104-+.
44. Chen, Z., et al., *Arbitrarily Accessible 3D Microfluidic Device for Combinatorial High-Throughput Drug Screening.* Sensors (Basel), 2016. **16**(10).
45. Santos, J.M., et al., *Red Blood Cell Invasion by the Malaria Parasite Is Coordinated by the PfAP2-I Transcription Factor.* Cell Host Microbe, 2017. **21**(6): p. 731-741 e10.
46. Wellems, T.E., et al., *'Artemisinin Resistance': Something New or Old? Something of a Misnomer?* Trends in Parasitology, 2020. **36**(9): p. 735-744.
47. Trager, W. and J.B. Jensen, *Human malaria parasites in continuous culture.* Science, 1976. **193**(4254): p. 673-5.
48. Miao, J. and L. Cui, *Rapid isolation of single malaria parasite-infected red blood cells by cell sorting.* Nat Protoc, 2011. **6**(2): p. 140-6.
49. Deitsch, K., C. Driskill, and T. Wellems, *Transformation of malaria parasites by the spontaneous uptake and expression of DNA from human erythrocytes.* Nucleic Acids Res, 2001. **29**(3): p. 850-3.
50. Miao, J., et al., *The Puf-family RNA-binding protein PfPuf2 regulates sexual development and sex differentiation in the malaria parasite Plasmodium falciparum.* J Cell Sci, 2010. **123**(Pt 7): p. 1039-49.
51. Liang, X., et al., *A Leak-Free Inducible CRISPRi/a System for Gene Functional Studies in Plasmodium falciparum.* Microbiol Spectr, 2022: p. e0278221.
52. Kim, D., B. Langmead, and S.L. Salzberg, *HISAT: a fast spliced aligner with low memory requirements.* Nat Methods, 2015. **12**(4): p. 357-60.

53. Anders, S. and W. Huber, *Differential expression analysis for sequence count data.* Genome Biol, 2010. **11**(10): p. R106.
54. Liao, Y., G.K. Smyth, and W. Shi, *featureCounts: an efficient general purpose program for assigning sequence reads to genomic features.* Bioinformatics, 2014. **30**(7): p. 923-30.
55. Smilkstein, M., et al., *Simple and inexpensive fluorescence-based technique for high-throughput antimalarial drug screening.* Antimicrobial Agents and Chemotherapy, 2004. **48**(5): p. 1803-1806.
56. Wang, Z.L., et al., *Artemisinin Resistance at the China-Myanmar Border and Association with Mutations in the K13 Propeller Gene.* Antimicrobial Agents and Chemotherapy, 2015. **59**(11): p. 6952-6959.
57. Witkowski, B., et al., *Novel phenotypic assays for the detection of artemisinin-resistant Plasmodium falciparum malaria in Cambodia: in-vitro and ex-vivo drug-response studies.* Lancet Infectious Diseases, 2013. **13**(12): p. 1043-1049.
58. Siddiqui, F.A., et al., *Plasmodium falciparum Falcipain-2a Polymorphisms in Southeast Asia and Their Association With Artemisinin Resistance.* Journal of Infectious Diseases, 2018. **218**(3): p. 434-442.
59. Straimer, J., et al., *Plasmodium falciparum K13 Mutations Differentially Impact Ozonide Susceptibility and Parasite Fitness In Vitro.* Mbio, 2017. **8**(2).
60. Siddiqui, F.A., et al., *Role of Plasmodium falciparum Kelch 13 Protein Mutations in P. falciparum Populations from Northeastern Myanmar in Mediating Artemisinin Resistance.* mBio, 2020. **11**(1).

FIGURE LEGENDS

Figure 1. KD of PfGCN5 led to parasite growth defects and increased susceptibilities to stress conditions. **A**. A diagram illustrates the TetR-DOZI inducible KD system, where 10x aptamer motifs are inserted into the 3' UTR of the *PfGCN5*. Adding aTc causes TetR-DOZI to be released from the aptamer, inducing protein translation (translation "ON"), whereas withdrawal of aTc leads to the binding of TetR-DOZI to the aptamer motifs to block the translational process (translation "OFF"), “AAAAA” indicates the polyA tail of the mRNA. **B**. Measurement of GFP expression in the TetR-PfGCN5:GFP parasites by flow cytometry. The reduction of PfGCN5-GFP protein level after withdrawal of aTc for 48 h is shown. **C**. The growth curves of TetR-PfGCN5:GFP parasites with or without aTc. The parasite growth rates were significantly reduced after KD of PfGCN5 (-aTc) compared to the parasites without KD of PfGCN5 (+aTc) ($p < 0.001$, multiple T-test). **D** and **E**. Parasite growth with or without *PfGCN5* KD exposed to heat shock (**D**) and low glucose (**E**) conditions, respectively. (**: $p < 0.01$, *** : $p < 0.001$, multiple T-test). TetR-PfGCN5:GFP parasites at the early ring stage with (+aTc) or without aTc (-aTc) were treated by HS (41 ºC) and low-glucose (0.5 g/L) for 6 h. aTc was added back to the culture after stress treatment. **F**. Parasite recovery assays showing the time required for the control (+aTC) or the PfGCN5 KD (-aTc) parasites to recover after treatment with 1 μM of DHA for 12 h ($p < 0.001$, multiple T-test). aTc was added back to the culture immediately after DHA treatment.

Figure 2. Transcriptional changes of +aTc TetR-PfGCN5::GFP parasites upon exposure to different stress conditions. **A-C**. Volcano plots showing differentially expressed genes at the ring stage after treatment with heat shock (HS) (**A**), low glucose (L-Glu) (**B**), and DHA (**C**). **D** and **E**. Venn diagrams showing the extent of overlaps among the up- (**D**) and down- (**E**) regulated genes upon HS, low glucose, and DHA treatments, respectively. **F** and **G**. Heatmaps display the GO enrichment analyses of up- (**F**) and down-(**G**) regulated genes upon HS, low glucose, and DHA treatments based on the biological process (BP), showing the common and stress-specific stress responses.

Figure 3. Transcriptomic analyses of PfGCN5-dependent stress responses. **A** and **B**. Venn diagrams showing the overlaps among the up- (**A**) and down- (**B**) regulated genes upon DHA, HS, and low-glucose treatments in the -aTc (PfGCN5 KD) parasites, respectively. **C**. Heatmaps show the expression patterns (Exp) in WT (+aTc) and PfGCN5 KD (-aTc) parasites upon HS, low glucose (L-Glu), and DHA treatments. ↑, ↓, and − denote genes that were up-, down-, and not-altered after treatments, ↗ indicates the genes failed to be up-regulated in PfGCN5 KD parasite after ART treatment. #: numbers of genes in each cluster. **D**. GO enrichment analyses of genes in different clusters. The GO terms shared among the three stress conditions are shown in bold and black color, while stress-specific enrichments are listed by words in red, blue, and green for HS, low glucose, and DHA treatments, respectively.

Figure 4. KD or inhibitor of PfGCN5 sensitized the parasites to DHA treatments. **A**. RSA of +aTc and -aTc parasites (TetR-PfGCN5::GFP) indicates that KD of PfGCN5 by the withdrawal of aTc (-aTc) led to the reduction of RSA values ($p < 0.01$, T-test). RSAs of +aTc parasite (~0.3%) were set up as 100% for comparison. aTc was added back to the culture after 6 h treatment by 700nM DHA. **B** and **C**. RSA of an ART-resistant K13 mutant strain (isolated from Cambodia with C580Y mutation) while MB-3 was added and withdrawn at the same time as DHA treatment. MB-3 at the concentrations of IC_{10} (10.9 μM), IC_{25} (17.3 μM), and IC_{50} (27.5 μM) without DHA did not cause any noticeable alteration of RSA value as compared to DMSO vehicle control (**C**) whereas co-incubation with both DHA and MB-3 significantly reduced RSA rate compared to DHA treatment only (**D**) (**: $p < 0.01$, *** : $p < 0.001$, T-test).

Figure S1. PfGCN5 knockdown using the TetR-DOZI system. **A.** Schematic diagram shows the insert of 10 x aptamer (A*) in 3' UTR of *PfGCN5* and integration of the TetR-DOZI expression cassette by single-crossover homologous recombination. KAT, lysine acetyltransferase domain; ADA2, ADA2-binding domain; BrD, bromodomain; H, HindIII restriction site. The recombined PfGCN5 locus includes GFP tagging at the C-terminus of PfGCN5. **B.** Southern blot indicates three positive clones from transfected parasites. M, molecular markers in Kb. **C.** Recovery of PfGCN5-GFP expression after adding aTc back to the KD parasite culture for 2-10h. The KD parasites were cultured without aTc (-aTc) for 5 IDCs before adding aTc. The PfGCN5-GFP

expression was measured by detecting the GFP level in the parasites via flow cytometry. The median GFP levels of 5000 parasites were used for each replicate. The percentage of GFP level compared to parasite cultured without withdrawal of aTc (+aTc). **D**. The growth rates of parasites without KD of PfGCN5 (+aTc) and parasites with re-storage of PfGCN5 expression by adding aTc back to the -aTc parasites (+aTc post KD). **E**. Growth recovery assays after 1μM of DHA treatment of 3D7 with and without –aTc.

Figure S2. Drastic transcriptional changes upon stress conditions. **A** and **B**. Heatmaps display the GO enrichment analyses of up- (**A**) and down- (**B**) regulated genes upon HS and low glucose (L-Glu), and DHA treatments based on the cellular component (CC) showing the common and stress-specific stress responses.

Figure S3. Overlaps among the genes in cluster I-V. A-E. Overlapping pie charts show the levels of overlaps among genes in clusters I-V upon DHA, HS, and low-glucose treatments, respectively.

Table S1. The transcriptomic changes in +aTc TetR-PfGCN5:GFP parasites at the ring stage under stress conditions.

Table S2. The transcriptomic changes in TetR-PfGCN5:GFP parasites at the ring stage after KD of PfGCN5.

Table S3. The transcriptomic changes in -aTc TetR-PfGCN5:GFP parasites at the ring stage under stress conditions.

Table S4. Expression patterns by comparing -aTc and +aTc TetR-PfGCN5:GFP parasites under three stress conditions.

Figure 1

A.

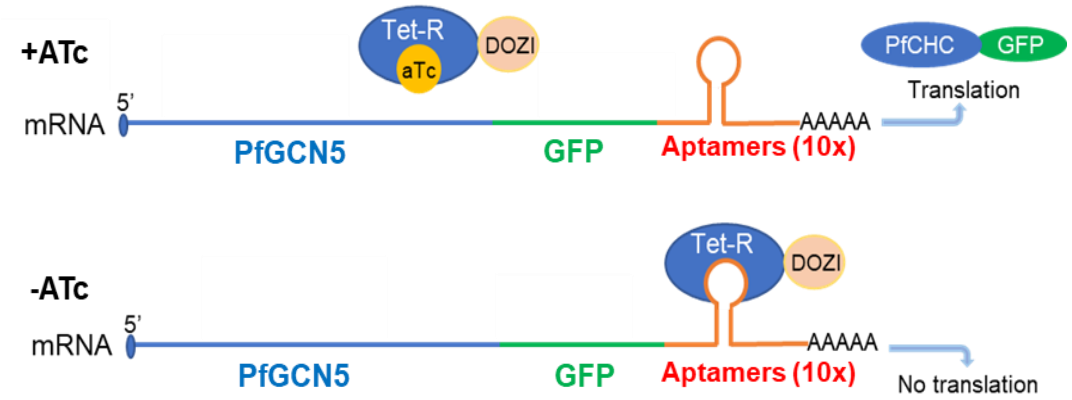

B.

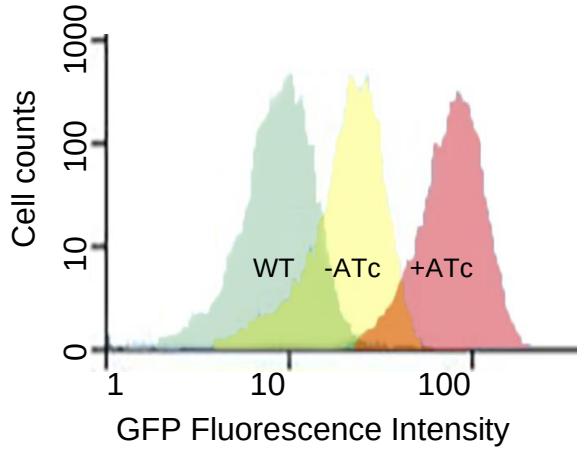

C.

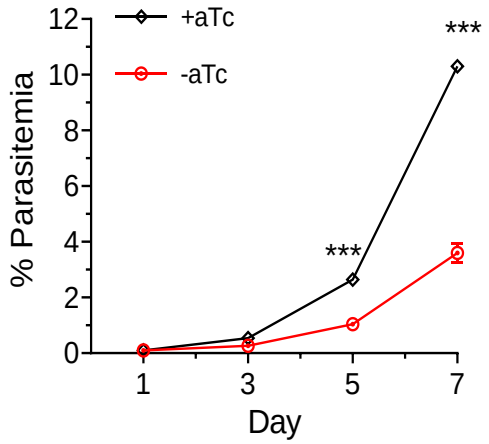

D.

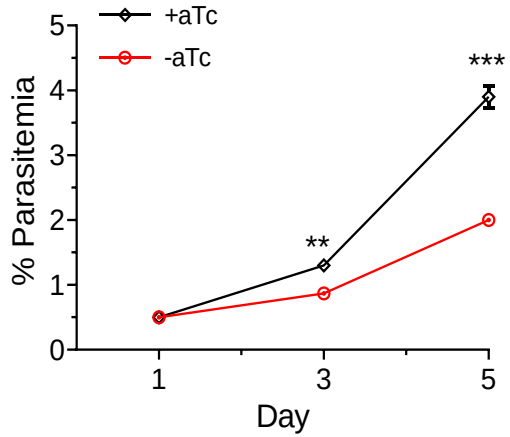

E.

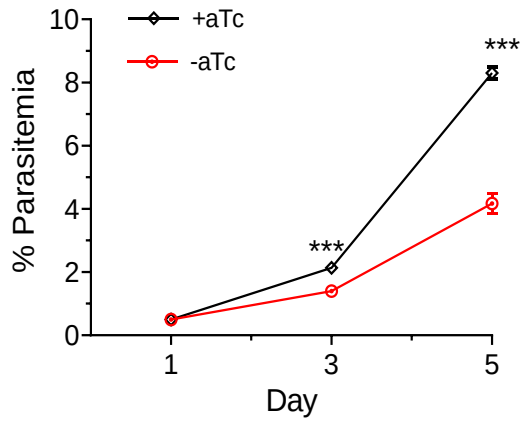

F.

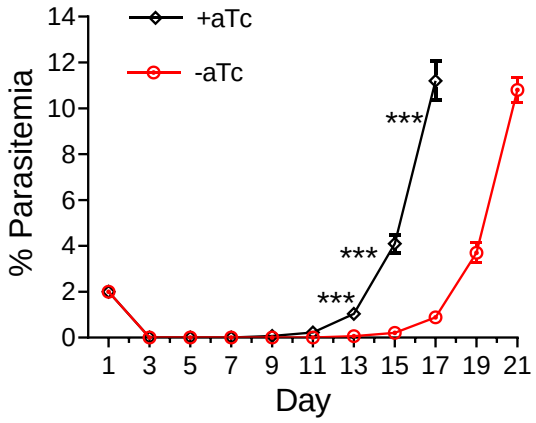

Figure 2

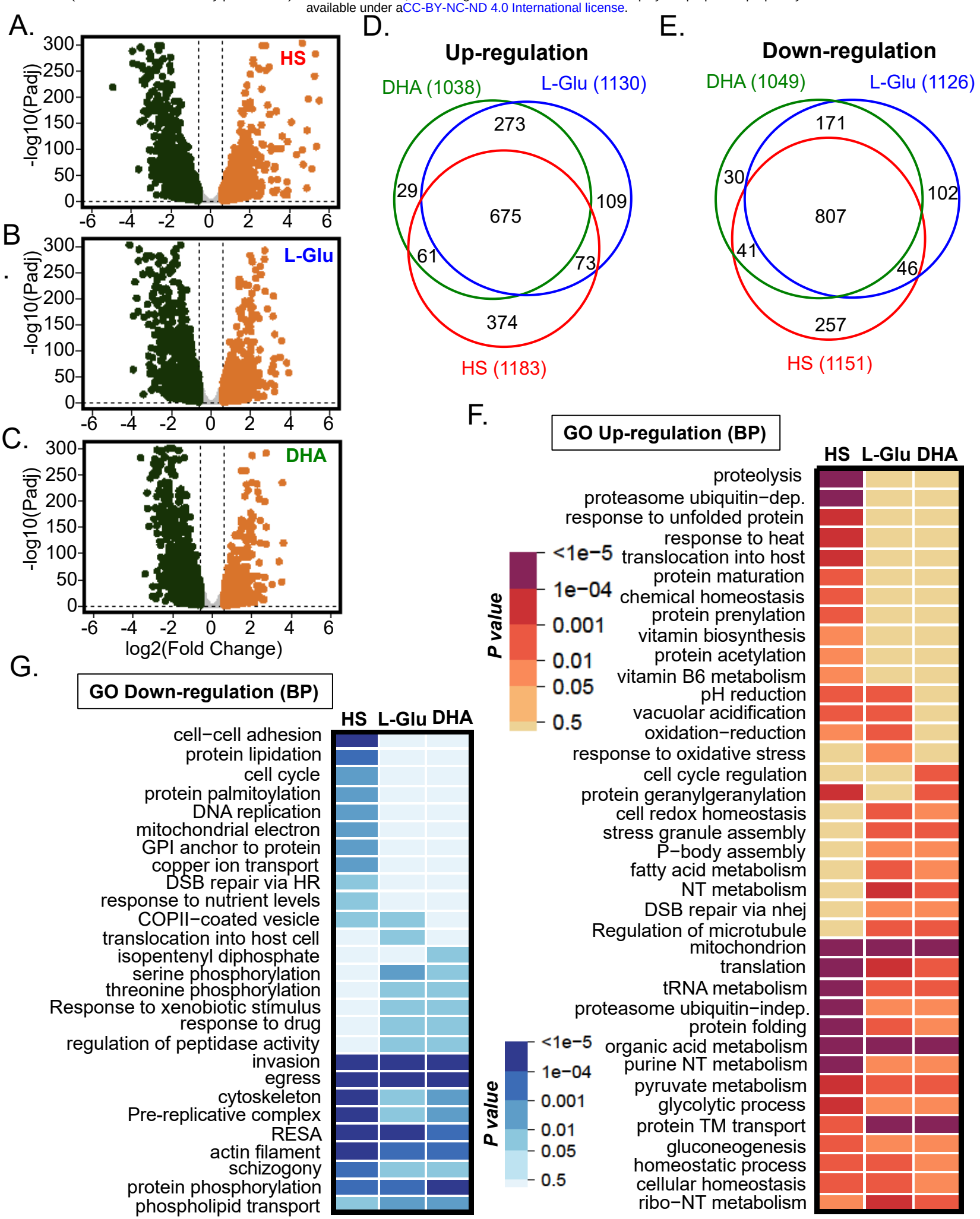

Figure 3

A.

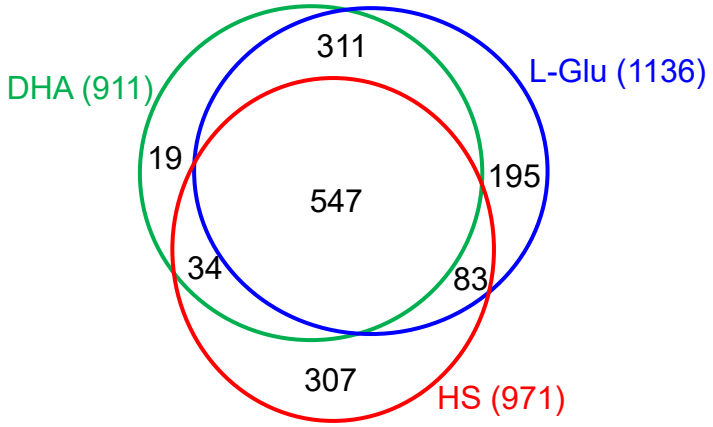

B.

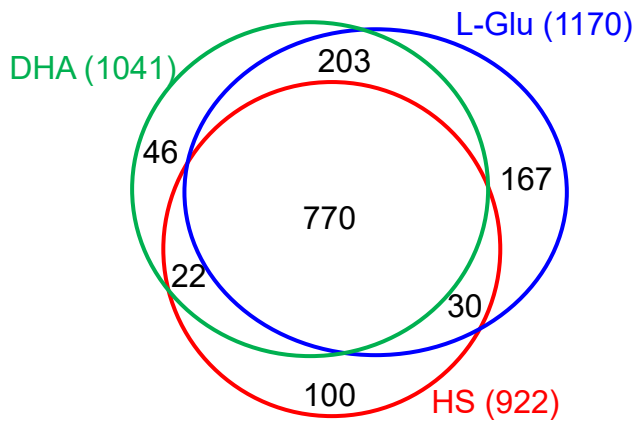

C.

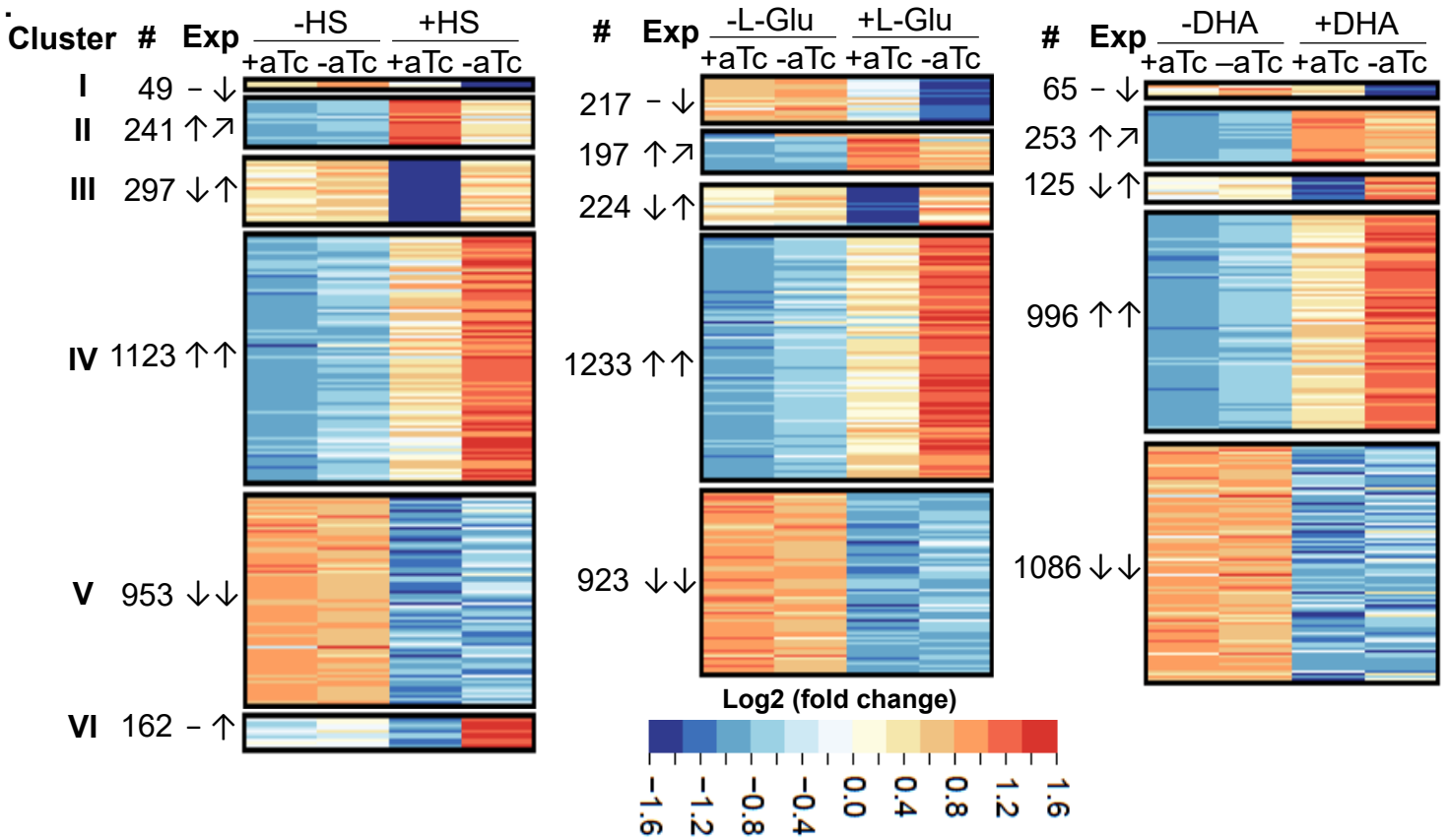

D.

Cluster — Heat shock, Low glucose, DHA treatment

Cluster	
I	**Ribosome biogenesis, GCN5, H3K4me3, response to drug, glutamine metabolism (KIC4)** HSP70 chaperone cycle, P-bodies, PTEX translocon, translation initiation
II	**Translation and ribosome, protein folding, tRNA process, ATP metabolic process, glycolysis, gluconeogenesis, ART proteome, response to drug xenobiotic stimulus, GARP, food vacuole, Sec61, PTEX translocon** Protein geranylgeranylation, proteasome assembly, mitochondrion transport and targeting, isoprenoid biosynthesis Cation homeostasis and pH reduction Hemoglobin digestion
III	**DNA replication and repair, cell cycle, isoprenoid biosynthesis, SERA** Cell adhesion, cytoskeleton organization, Mitochondrion electron transport
IV	**Proteasome, protein folding, mitochondrion, apicoplast, stress granule assembly, cytoskeleton organization, transport, fatty acid synthesis, gametocyte proteomics, ERAD** Response to heat and oxidative stress, ERAD, tRNA, amino acid and vitamin B6 metabolism, protein geranylgeranylation, microtube-based movement, cation homeostasis and pH reduction Response to ER stress and abiotic stimulus, cell redox homeostasis, cell cycle
V	**Entry into and exit from host, actin filament-based movement, endocytosis, protein modifications, food vacuole** Response to drug, lipid metabolic process Response to starvation, mRNA process, vesicle organization Response to drug and xenobiotic stimulus

Figure 4

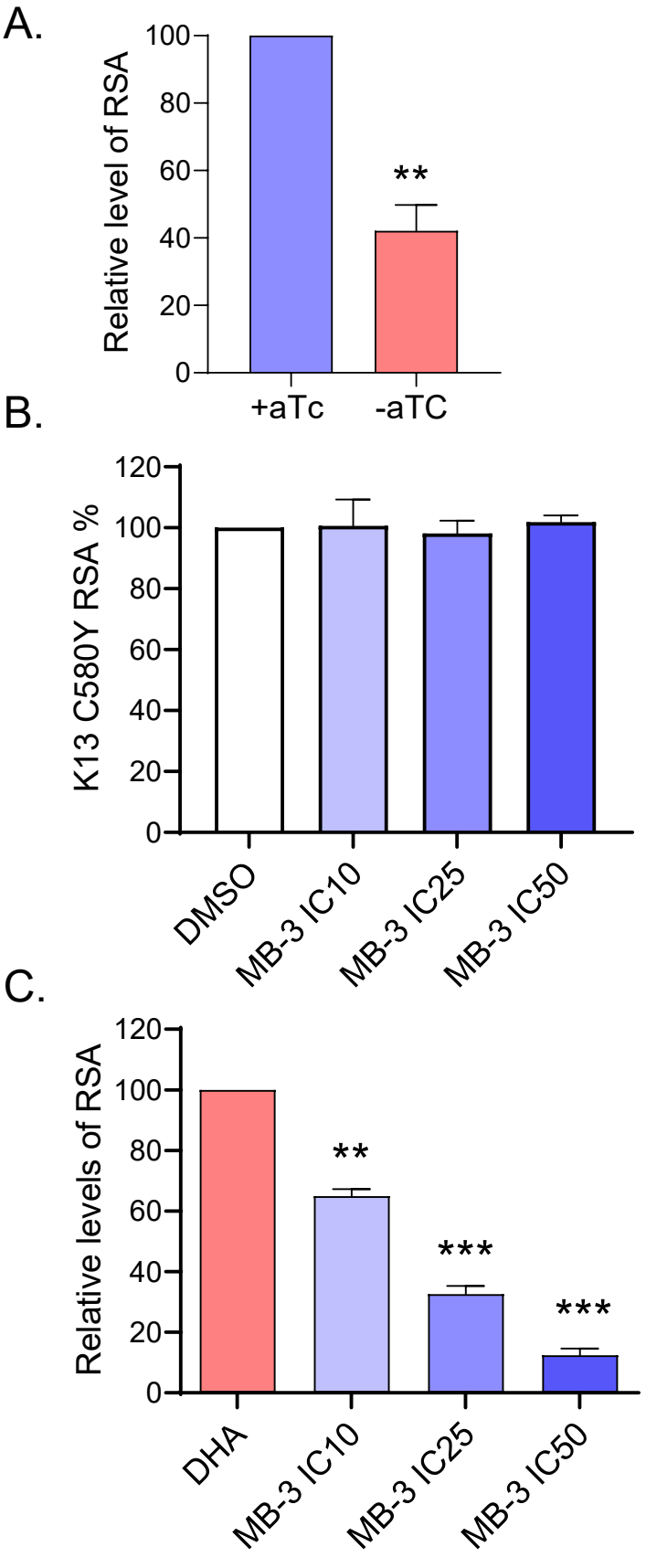
A.
Relative level of RSA
100
80
60
40
20
0
**
+aTc
-aTC
B.
K13 C580Y RSA %
120
100
80
60
40
20
0
DMSO
MB-3 IC10
MB-3 IC25
MB-3 IC50
C.
Relative levels of RSA
120
100
80
60
40
20
0
**
***
***
DHA
MB-3 IC10
MB-3 IC25
MB-3 IC50